Clin Pharmacokinet (2014) 53:89–102
DOI 10.1007/s40262-013-0090-5

ORIGINAL RESEARCH ARTICLE

Development of a Paediatric Population-Based Model of the Pharmacokinetics of Rivaroxaban

Stefan Willmann · Corina Becker · Rolf Burghaus · Katrin Coboeken · Andrea Edginton · Jörg Lippert · Hans-Ulrich Siegmund · Kirstin Thelen · Wolfgang Mück

Published online: 3 August 2013

Abstract

Background Venous thromboembolism has been increasingly recognised as a clinical problem in the paediatric population. Guideline recommendations for antithrombotic therapy in paediatric patients are based mainly on extrapolation from adult clinical trial data, owing to the limited number of clinical trials in paediatric populations. The oral, direct Factor Xa inhibitor rivaroxaban has been approved in adult patients for several thromboembolic disorders, and its well-defined pharmacokinetic and pharmacodynamic characteristics and efficacy and safety profiles in adults warrant further investigation of this agent in the paediatric population.

Objective The objective of this study was to develop and qualify a physiologically based pharmacokinetic (PBPK) model for rivaroxaban doses of 10 and 20 mg in adults and to scale this model to the paediatric population (0–18 years) to inform the dosing regimen for a clinical study of rivaroxaban in paediatric patients.

Methods Experimental data sets from phase I studies supported the development and qualification of an adult PBPK model. This adult PBPK model was then scaled to the paediatric population by including anthropometric and physiological information, age-dependent clearance and age-dependent protein binding. The pharmacokinetic properties of rivaroxaban in virtual populations of children were simulated for two body weight-related dosing regimens equivalent to 10 and 20 mg once daily in adults. The quality of the model was judged by means of a visual predictive check. Subsequently, paediatric simulations of the area under the plasma concentration–time curve (AUC), maximum (peak) plasma drug concentration (C_{max}) and concentration in plasma after 24 h (C_{24h}) were compared with the adult reference simulations.

Results Simulations for AUC, C_{max} and C_{24h} throughout the investigated age range largely overlapped with values obtained for the corresponding dose in the adult reference simulation for both body weight-related dosing regimens. However, pharmacokinetic values in infants and preschool children (body weight <40 kg) were lower than the 90 % confidence interval threshold of the adult reference model and, therefore, indicated that doses in these groups may need to be increased to achieve the same plasma levels as in adults. For children with body weight between 40 and 70 kg, simulated plasma pharmacokinetic parameters (C_{max}, C_{24h} and AUC) overlapped with the values obtained in the corresponding adult reference simulation, indicating that body weight-related exposure was similar between these children and adults. In adolescents of >70 kg body weight, the simulated 90 % prediction interval values of AUC and C_{24h} were much higher than the 90 % confidence interval of the adult reference population, owing to the weight-based simulation approach, but for these patients rivaroxaban would be administered at adult fixed doses of 10 and 20 mg.

Conclusion The paediatric PBPK model developed here allowed an exploratory analysis of the pharmacokinetics of

Electronic supplementary material The online version of this article (doi:10.1007/s40262-013-0090-5) contains supplementary material, which is available to authorized users.

S. Willmann (✉) · K. Coboeken · J. Lippert · H.-U. Siegmund · K. Thelen
Bayer Technology Services GmbH, Leverkusen, Germany
e-mail: stefan.willmann@bayer.com

C. Becker · R. Burghaus · W. Mück
Bayer HealthCare AG, Wuppertal, Germany

A. Edginton
University of Waterloo, Waterloo, ON, Canada

rivaroxaban in children to inform the dosing regimen for a clinical study in paediatric patients.

1 Introduction

In recent years, venous thromboembolism (VTE) has been increasingly recognised as a clinical problem in the paediatric population. It is associated with significant morbidity and mortality in those affected, especially children with severe underlying conditions (such as cancer) and multiple risk factors [1–3]. In the general paediatric population, the incidence of VTE is low, occurring at a rate of 0.06–0.14 per 10,000/year [4, 5]. However, in hospitalised children a significantly higher incidence of VTE was reported. A study conducted in the early 1990s in Canada demonstrated an incidence of VTE among paediatric patients of 5.3 per 10,000 admissions/year [6]. In a US paediatric study over a period of 7 years, the incidence of VTE increased from 34 to 58 cases per 10,000 admissions/year [1], with neonates and adolescents being at the greatest risk [1, 7]. Whether these data indicate a true increase in occurrence of VTE in the paediatric population (potentially influenced by improved survival chances of seriously ill paediatric patients owing to medical advances) or an increase in detection of previously undiagnosed VTE remains unclear. Major physiological changes in the haemostatic system throughout childhood are well documented and affect the frequency and natural history of VTE in children [8]. These changes will also affect the response of children to anticoagulants [8].

Guidelines from the American College of Chest Physicians recommend the use of unfractionated heparin, low-molecular-weight heparin and vitamin K antagonists for the prevention and treatment of VTE in children [8]. These guidelines are based mainly on extrapolation from results of clinical trials conducted in adults because ethical and technical issues have limited the number of clinical trials in paediatric populations. Therefore, in clinical practice, there is a high level of off-label use of drugs in children: 50 % of drugs that are administered to children have not been tested in the appropriate age group [9–14]; this number increases to up to 90 % of drugs administered to preterm and term babies admitted to neonatal intensive care units [12, 13].

Rivaroxaban is an oral, direct Factor Xa inhibitor that has been shown to exhibit well-defined pharmacokinetic and pharmacodynamic properties, with high oral bioavailability (>80 %) and limited food and drug interactions in healthy adults [15–22]. Rivaroxaban inhibits free and fibrin-bound Factor Xa as well as Factor Xa in the prothrombinase complex and, therefore, prevents clot formation and clot growth [23]. Rivaroxaban has been widely studied in phase III clinical trials involving more than 60,000 adult patients and, based on these results, has been approved in adults for the prevention of VTE after elective hip or knee replacement surgery [24–27]; the treatment of acute, symptomatic deep vein thrombosis, treatment of acute pulmonary embolism and prevention of recurrent VTE [28, 29]; and the prevention of stroke and systemic embolism in patients with non-valvular atrial fibrillation [30]. Rivaroxaban has also successfully completed a phase III clinical trial for secondary prevention of cardiovascular events in patients after acute coronary syndrome [31].

Owing to its well-defined pharmacokinetic and pharmacodynamic properties and its efficacy and safety profiles in adults, rivaroxaban warrants investigation in children. There are currently no data on the use of rivaroxaban in children; however, oral suspensions of rivaroxaban 10 and 20 mg (concentration 1 mg/mL), which have already been tested in phase I studies in healthy male adults, may be a suitable formulation for children because exact dosing is possible. It is anticipated that this oral formulation will form the basis of potential future paediatric use [32].

Current regulations from the US FDA and the European Medicines Agency request development strategies for paediatric dosing recommendations for drugs that have been approved in adults. These dosing strategies aim to maintain in children (<18 years of age) the efficacy and safety seen in adults [33]. Physiologically based pharmacokinetic (PBPK) modelling strategies have been used to predict dosing regimens for paediatric clinical trials by accounting for developmental changes that affect the absorption, distribution, metabolism and excretion of drugs [34]. Although pharmacodynamic modelling also plays a part, the modelling of pharmacokinetic parameters could directly inform dosing strategies in the paediatric population and, therefore, is considered the major component of paediatric modelling initiatives and, hence, is the focus of this article [33, 35]. Furthermore, the FDA highlights the need and value of PBPK modelling studies to improve the design of paediatric drug development studies with the ultimate aim of reducing off-label use of drugs in paediatric patients [35, 36].

The first objective of this study was to develop and qualify a PBPK model for rivaroxaban doses of 10 and 20 mg in adults and to scale this model to the paediatric population. The second objective was to predict the pharmacokinetic properties of rivaroxaban in children and to use this information to guide dosing in a paediatric phase I trial [ClinicalTrials.gov identifier: NCT01145859. http://clinicaltrials.gov/show/NCT01145859 (Accessed 19 July 2013)]. This trial is currently ongoing and is assessing the pharmacokinetics and pharmacodynamics of rivaroxaban in paediatric patients who have completed anticoagulant treatment for VTE, but who are considered to be at risk of VTE recurrence.

2 Methods

2.1 Data Sources

Experimental data sets from phase I studies [16, 32, 37] carried out in healthy adults (see Table 1 and the Electronic Supplementary Material: Section 1) were used to support the development and qualification of an adult PBPK model. In all studies, the rivaroxaban tablets administered were immediate-release formulations unless otherwise stated. Physiochemical data of rivaroxaban that were used in the model, including solubility, molecular weight and fraction unbound (i.e. plasma protein binding), are listed in Table 2.

2.2 Generic Workflow for Model Development

The generic workflow for the scaling of drug pharmacokinetics from adults to the paediatric population using PBPK modelling has been described previously and remained unchanged in this study (Fig. 1) [38].

2.3 Software Used

All PBPK simulations were carried out using the commercially available software PK-Sim® (Version 4.2, Bayer Technology Services, Leverkusen, Germany; http://www.systems-biology.com) and exported to MoBi® (Version 2.3, Bayer Technology Services, Leverkusen, Germany), where a novel model for gastrointestinal transit and absorption was added, which is part of PK-Sim® Version 5.0 and higher [39, 40].

All optimisations and batch mode simulations for MoBi models were carried out using MATLAB® [Version 7.11.0 (R2010b), The MathWorks Inc., Natick, MA, USA] and the MoBi Toolbox for MATLAB (Version 2.3 Bayer Technology Services, Leverkusen, Germany).

2.4 Physiologically Based Pharmacokinetic (PBPK) Model for Intravenous Administration in Adults

2.4.1 Lipophilicity

Data from the absolute bioavailability study [32] were used to modify the lipophilicity of rivaroxaban with the aim of adjusting the simulated plasma concentration–time curve based on the PBPK model to reflect the experimental data more closely, especially for the early distribution phase (Study B, Table 1). The partition coefficients were estimated using the method of Rodgers and Rowland [41–43].

2.4.2 Clearance Processes

The rivaroxaban PBPK model contains three hepatic, first-order clearance processes and two renal clearance processes. The first hepatic process describes the clearance of rivaroxaban via cytochrome P450 (CYP) 3A4/5; the second process describes the clearance of rivaroxaban via CYP2J2;

Table 1 Experimental data sets of phase I studies assessing the pharmacokinetics of rivaroxaban in healthy male adult subjects

Study	Topic	Main outcome
Study A	Mass balance and safety [37]	Rivaroxaban and its metabolites were eliminated via renal (66 %) and biliary/faecal routes (28 %)
Study B	Absolute bioavailability [32]	Compared with a 1 mg IV dose, under fasted conditions the bioavailability of rivaroxaban 5 mg was complete and was 66 % for rivaroxaban 20 mg. Bioavailability of rivaroxaban 20 mg was 59 % relative to the 5 mg dose
Study C	Pharmacokinetics across a wide dose range [16]	Rivaroxaban had well-defined pharmacokinetic characteristics across doses of 1.25–80 mg administered as oral solution or tablet
Study D	Absorption from proximal and distal small bowel and ascending colon	The relative bioavailability of rivaroxaban depends on the site of absorption along the gastrointestinal tract and is poorest in the ascending colon
Study E	Food effect on pharmacokinetics of two 5 mg tablets	Compared with fasted conditions, mean t_{max}, mean AUC and mean C_{max} of rivaroxaban 10 mg were increased when taken with food
Study F	Food effect on pharmacokinetics of four 5 mg tablets or one 20 mg tablet	There were no pharmacokinetic differences between the two dosing regimens or between two types of meals. Mean t_{max}, mean AUC and mean C_{max} were significantly higher after food
Study G	Food effect on pharmacokinetics of one 10 mg tablet or one 20 mg tablet	Bioavailability of rivaroxaban 10 mg was independent of food Bioavailability of rivaroxaban 20 mg was similar when taken with food and lower when taken without food
Study H	Food effect on pharmacokinetics of 10 mg and 20 mg oral solution	Bioavailability of rivaroxaban 10 mg was independent of food Bioavailability of rivaroxaban 20 mg was similar when taken with food and lower when taken without food

AUC area under the plasma concentration–time curve, C_{max} maximum (peak) plasma drug concentration, *IV* intravenous, t_{max} time to C_{max}

Table 2 Physiochemical data of rivaroxaban

Parameter	Reported value	Value used in this study
Lipophilicity		2.275
cLog P	2.39[a]	
cLog MA	2.39[a]	
Plasma protein binding in adults		
Plasma f_u	5.1 % [45]	5.1 %[b]
Solubility		
Water solubility	7 mg/L[b]	
Solubility in FaSSIF/used in fasted state	20 mg/L[b]	20 mg/L
Solubility in FeSSIF/used in fed state	80 mg/L[b]	80 mg/L
Molecular weight	435.89 g/mol[b]	435.89 g/mol
Intestinal permeability coefficient		
In the small intestine		4.74×10^{-6} cm/s
In the large intestine		9.48×10^{-6} cm/s

cLog MA calculated Log value of the membrane affinity, *cLog P* calculated Log value of the octanol water partition coefficient, *FaSSIF* fasted state simulated intestinal fluid, *FeSSIF* fed state simulated intestinal fluid

[a] Because no experimental lipophilicity value was available, the lipophilicity value had to be calculated in silico based on its chemical structure. The Bayer in-house cheminformatics tool (Pythia) was used for this purpose. Pythia requires the chemical structure as input (e.g. imported via MDL ISIS/Draw) and predicts, among other physicochemical properties, the Log MA value using a fragment-based quantitative structure–activity relationship (QSAR) method. The tool is embedded in a Bayer in-house software platform to calculate absorption, distribution, metabolism and excretion (ADME) properties

[b] Bayer HealthCare data on file

and the third hepatic process describes CYP-independent hydrolysis of rivaroxaban. Renal clearance processes include the glomerular filtration rate (GFR) and tubular secretion. Clearance percentages originally determined for oral administration according to mass balance and in vitro information were: 6 % GFR, 30 % tubular secretion, 7 % faecal unchanged, 18 % CYP3A4/5, 14 % CYP2J2, 14 % hydrolysis and 11 % unaccounted [37, 44, 45]. Faecal excretion was disregarded and the unaccounted part was assumed to be caused by hepatic clearance processes and proportionally distributed across the three hepatic processes. Based on the unbound fraction in plasma (f_u) of 5.1 % of rivaroxaban in adults, the contribution of glomerular filtration was approximately 6 mL/min (estimated from $\text{GFR} \times f_u = 120 \text{ mL/min} \times 0.051 = 6.1 \text{ mL/min}$) [37, 44–46]. To account for the renal clearance exceeding glomerular filtration, the tubular secretion was set at 30 mL/min, resulting in a total urinary excretion of 36 mL/min.

2.5 PBPK Model for Oral Administration in Adults

After establishing the intravenous PBPK model in adults, the model was expanded to account for oral administration of rivaroxaban. To improve description of the absorption process, a recently developed compartmental model for gastrointestinal transit and absorption was implemented [39, 40].

For the simulations of the effect of food on pharmacokinetics of orally administered rivaroxaban in adults, the meal energy content was uniformly distributed between 593 kcal (corresponding to a high-carbohydrate "continental" breakfast [18]) and 1,051 kcal (corresponding to a high-fat, high-calorie "American" breakfast [18]) for the simulation of fed conditions. For both meals, solid and liquid components were estimated to be equal, i.e. 50 % each. For adults, the gastric emptying time under fed conditions was fitted to experimental data taken from the food effect study of rivaroxaban 10 mg (administered as two 5 mg tablets). According to this function, emptying from the stomach is slow during the first 2 h and then accelerates so that emptying is almost complete 5 h after drug administration [47, 48].

All other compound-specific parameters (including the adjusted lipophilicity parameter) and clearance were the same as in the intravenous model. The permeability coefficient for the small intestine was determined based on results from the orally administered solution (Study C, Table 1), and the permeability coefficient for the large intestine was based on the absorption site study (Study D, Tables 1, 2). The dissolution behaviour of the rivaroxaban tablets was then considered via the dissolution module of PK-Sim® that incorporates a Noyes–Whitney module for spherical particles into the gastrointestinal transit and absorption model [49, 50]. This module allows for the dynamic simulation of particle size-dependent dissolution in an environment that changes during transit through the gastrointestinal tract (e.g. pH, solubility). A more detailed description of this add-on module has been published [50]. Owing to absorption being dependent on particle size, it is noteworthy that both suspension and tablet formulations contain the same micronised drug. For rivaroxaban, monodisperse particles with a median diameter of 3 µm (according to the specification of the powder), a diffusion coefficient of 4.9×10^{-5} cm^2/s (fitted to experimental data [16]) and a diffusion layer thickness of 20 µm (PK-Sim® default) were assumed.

For model qualification, population simulations in an adult reference population were performed for 10 and 20 mg tablets first under fasted and then under fed conditions and compared with independent experimental data sets. Further, experimental data obtained in adults after administration of rivaroxaban 10 and 20 mg as oral

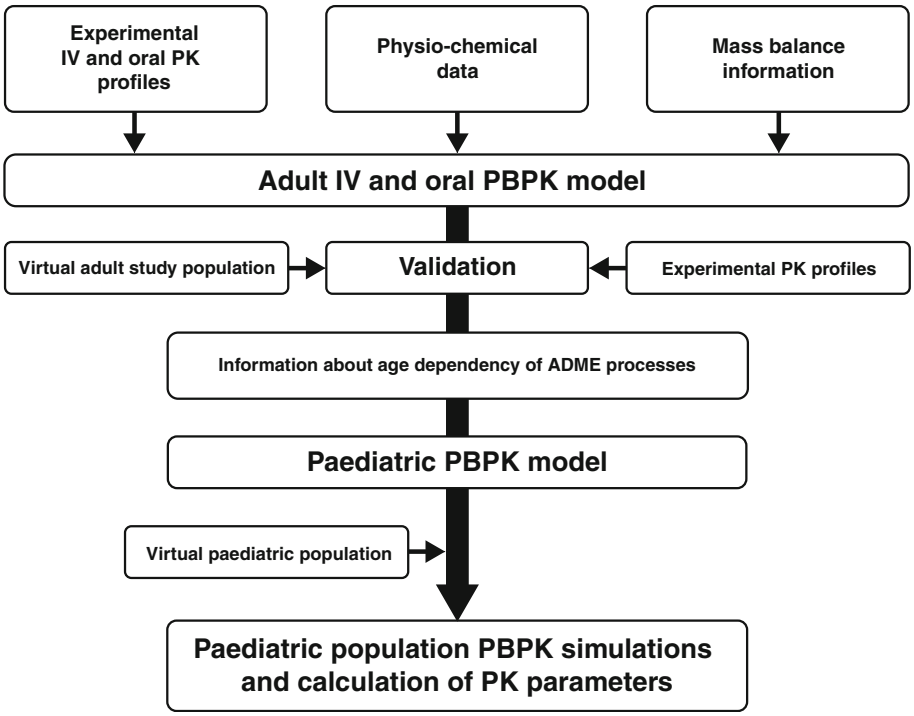

Fig. 1 Generic workflow for the PBPK-based scaling of rivaroxaban pharmacokinetics from adults to children. *ADME processes* processes that involve absorption, distribution, metabolism and excretion of a drug, *IV* intravenous, *PK* pharmacokinetic, *PBPK* physiologically based pharmacokinetic

suspension under fasting conditions and 20 mg under fed conditions were compared with simulations in an adult reference population. The quality of the adult model was judged by means of a visual predictive check (VPC), a popular tool for evaluating the performance of population pharmacokinetic/pharmacodynamic models. The VPC compares different percentiles of the experimental data with percentiles of simulated data [51, 52].

2.6 Rivaroxaban Doses Used in the Paediatric Simulations

For paediatric simulations, body weight-adjusted doses of rivaroxaban were used. Doses for paediatric simulations were derived from adult doses assuming a typical body weight of 70 kg for adults. Thus, a paediatric dose of 0.143 mg/kg body weight is equivalent to a 10 mg dose in adults, and a paediatric dose of 0.286 mg/kg body weight is equivalent to a 20 mg adult dose.

2.7 Scaling of the Adult PBPK Model to Children

Using the adult PBPK model as a basis, the model was scaled to children by including anthropometric and physiological information, age-dependent clearance and age-dependent protein binding. Simulations with virtual populations of children from term neonates (assuming a birth weight of ≥2 kg) to adolescents aged 18 years were carried out. No further changes to any other input parameters (e.g. specific intestinal permeability, solubility) were made in comparison with the adult reference model.

2.7.1 *Anthropometric and Physiological Information*

The model was scaled taking into account age-dependent parameters of height and body weight and physiological parameters (blood flow, organ volumes, binding protein concentration, haematocrit, cardiac output) in children in line with previously published data [34]. This information is incorporated into PK-Sim® and was used as default values for the simulations in children.

2.7.2 *Clearance Scaling*

The clearances, as defined and quantified in the adult PBPK model, were scaled as published previously [53]. In brief, clearance scaling was based on developmental changes regarding the major enzymes that catalyse clearance processes. When developmental changes of a clearance process were not available, enzyme activity was scaled in comparison with adult activity on a per-organ weight basis. Calculations of intrinsic clearances from plasma clearances and plasma clearances from intrinsic clearances were made using the well-stirred model [54, 55]. Age-dependent parameters in children (including height, body weight, blood flow, organ volumes, binding protein concentration, haematocrit and cardiac output) were used, as previously published [53], and were incorporated as default values.

2.7.3 Protein Binding

Developmental changes in the concentration of human serum albumin in plasma were used to scale f_u, as described previously [34, 56].

2.7.4 Net Tubular Secretion

Net tubular secretion of rivaroxaban was scaled, assuming that the major transport protein was P-glycoprotein (P-gp). P-gp is an adenosine triphosphate-dependent efflux pump, the ontogeny of which has not been explicitly studied in humans. Studies in mice and rats have shown inconsistent results for expression levels of P-gp in the kidney at birth (11–96 %) and the postnatal age when adult expression levels were reached (0–21 days) [57–59].

Owing to the fact that digoxin is a P-gp substrate and is primarily cleared via P-gp-mediated tubular secretion and GFR in the kidney [59], digoxin renal clearance was used to estimate the ontogeny of the P-gp transporter in the kidney of humans. Adult renal clearance values for digoxin are approximately 2.5 mL/min/kg [60, 61], and values across the age groups of term neonates to 18 years are available in the literature [62–65]. Because renal clearance of digoxin is the sum of GFR and net tubular secretion, GFR (as calculated from Edginton et al. [53]) was subtracted from total renal clearance for each data point to calculate the age-dependence of tubular secretion via P-gp.

2.7.5 Absorption from the Gastrointestinal Tract

For the purpose of modelling, rivaroxaban was assumed to be given to children either in the fasted state with water or in the fed state after ingestion of an intermediate- to high-calorie meal. The fasted and fed states were simulated separately and the results were then merged to represent in vivo conditions. This approach allows mimicking of the range of feeding states as expected in hospitalised children, including those randomised for the paediatric phase I trial (NCT01145859).

For simulations across the paediatric age range, assumptions and values for the gastric emptying time, specific intestinal permeability (i.e. the intestinal permeability normalised to the surface area), the pH of the gastrointestinal tract, small intestinal transit times and the intestinal surface area were used as specified in Table 3 (see also the Electronic Supplementary Material: Section 2 for more detailed information).

2.7.6 Establishment of the Virtual Paediatric Population

Virtual paediatric populations were created using the population module of PK-Sim® [66, 67]. Twenty-eight age groups were considered (ages of 0 days, 3 days, 7 days, 14 days, 1 month, 2 months, 3 months, 6 months, 9 months, 1 year, 1.5 years, and then each year from 2 to 18 years), each consisting of 250 fasted male, 250 fed male, 250 fasted female and 250 fed female children (i.e. a total of 1,000 children per age group). The population module created virtual individuals within a given age, body weight and body height or body mass index range on a stochastic approach using age-dependent distributions of demographic and physiological parameters. The details of this algorithm and the sources for the empirical physiological distributions have been published previously [66, 67].

The mean intrinsic clearances, as calculated for each age group, were assigned to each virtual individual first and then subsequently randomised using variation measures from literature-based in vitro experiments [48, 62, 68–86]. Assumptions and values used for the randomisation of CYP3A4, CYP2J2, CYP-independent hydrolysis, GFR, the kidney P-gp transporter, gastric emptying time in the fasted and the fed state, transit times of the small and the large intestine and effective surface area of intestinal sections are shown in Table 3. Simulations in children for the fasted and fed states were carried out separately and subsequently pooled for the analysis to mimic the expected conditions in the paediatric clinical trial (NCT01145859).

3 Results

The previously proposed step-wise approach (Fig. 1) was used to adjust PBPK model parameters based on experimental data in adults for intravenous and oral administration of rivaroxaban. The parameters were then scaled and adjusted for paediatric populations. Based on this PBPK model, simulations in paediatric populations were performed for pharmacokinetic parameters after oral administration of doses equivalent to rivaroxaban 10 mg/70 kg (low dose equivalent to 0.143 mg/kg) body weight and rivaroxaban 20 mg/70 kg (high dose equivalent to 0.286 mg/kg) body weight.

3.1 Development and Verification of a PBPK Model for Intravenous and Oral Rivaroxaban in Adults

3.1.1 Intravenous PBPK Model

The plasma concentration–time profile of rivaroxaban after intravenous administration was plotted using data from the absolute bioavailability study [32]. This plot was overlaid with results simulated by the PBPK reference model. A monoparametric fit identified a lipophilicity value of LogP = 2.275. Experimental data were described

Table 3 Assumptions and values used for the randomisation of factors used in the study, based on data from in vitro experiments

Factor	Assumption	References
CYP3A4	Log-normal distribution with a geometric SD of 1.5 (average value of the SDs reported in the literature)	[68, 71, 72]
CYP2J2	Log-normal distribution with a geometric SD of 2.5 (based on the CYP2J2 mRNA distribution in postnatal liver samples)	[69]
CYP-independent hydrolysis	Log-normal distribution and a geometric SD of 1.3 (assumed empirical value)	
Renal clearance via GFR	By use of the equation below, three normal-distributed random variables were obtained: Hill coefficient = 15 ± 0.257, TM_{50} = 44.4 ± 1.04 weeks, and GFR_{mat} = 266 ± 60.7 min^{-1}	[70]
	$GFR = \left(\left(\frac{PMA^{Hill}}{TM_{50}^{Hill} + PMA^{Hill}} \cdot (1 - GFR_{premat}) \right) + GFR_{premat} \right) \cdot Volume_{Kidney} \cdot GFR_{mat}$	
Active renal secretion via kidney P-gp transporter[a]	Log-normal distribution and a geometric SD of 1.3	[62]
Gastric emptying time in the fasted state	Log-normal distribution with a geometric SD of 1.6 (based on data of more than 100 experimental gastric emptying profiles; data also used for the evaluation of the ontogeny)	[48, 73–75]
Gastric emptying time in the fed state	More than 100 experimental gastric emptying profiles that were obtained in healthy adults after ingestion of meals with an energy content of 593–1,051 kcal were used for the parameterisation of the gastric emptying time function of the Weibull type assuming a log-normal distribution of the parameters α and β, with geometric SDs of 1.74 in the case of α and 1.32 for β:	[48]
	$A(\text{time}) = A_0 \times e^{\frac{-\text{time}\beta}{\alpha}}$	
	The identical randomisation was done in children	
Small intestinal transit time	Log-normal distribution with a geometric SD of 1.6	[76–82]
Large intestinal transit time	Log-normal distribution with a geometric SD of 1.6 based on literature data	[83, 84]
Effective surface area of intestinal sections	Log-normal distribution with a geometric SD of 1.6 (applies to all intestinal sections)	[85, 86]

[a] Rivaroxaban is a P-gp substrate

A amount of drug/volume of meal, A_0 initial amount of drug/initial amount of meal, α optimised parameter depending on meal energy content (kcal), *β* optimisation parameter related to the fraction of solid components of the meal, *CYP* cytochrome P450, *e* exponent, *GFR* glomerular filtration rate, GFR_{mat} GFR after maturity, GFR_{premat} GFR during development, *P-gp* P-glycoprotein, *PMA* postmenstrual age, *SD* standard deviation, TM_{50} maturation half time

sufficiently accurately when simulating the pharmacokinetics of rivaroxaban after intravenous administration with this lipophilicity value (Fig. 2). This was particularly obvious in the infusion phase and the early distribution phase after discontinuation of the infusion. The adjusted lipophilicity parameter was used for all further simulations.

3.1.2 *Oral PBPK Model for Solution and Tablet Formulations of Rivaroxaban*

After establishing the intravenous PBPK model for rivaroxaban in adults, the model was expanded to simulate absorption from the gastrointestinal tract after oral administration of rivaroxaban. The experimental plasma

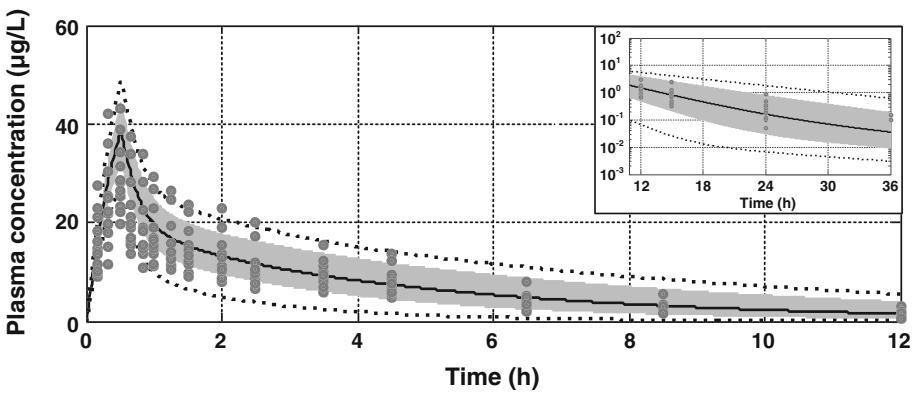

Fig. 2 Individually observed (*dots*) and simulated (*lines*) plasma concentration–time profiles for rivaroxaban after a 30-min intravenous infusion of 1 mg rivaroxaban in healthy adults depicted as a linear (*main graph*) and semi-log plot (*inset*). Simulated data are represented as geometric means (*black line*), 90 % prediction interval (*grey shaded area*) and minimum and maximum values (*dotted lines*)

concentration–time data obtained after administration of oral solutions containing rivaroxaban 5 or 10 mg to fasted healthy volunteers were used to identify the specific small intestinal permeability. The specific large intestinal permeability was obtained from the data obtained in a study, in which the Enterion™ capsule was used for site-specific administration of rivaroxaban in various regions of the gastrointestinal tract [87]. The intestinal permeability coefficients were adjusted to 4.74×10^{-6} cm/s for the small intestine and 9.48×10^{-6} cm/s for the large intestine. Simulations of plasma concentration–time profiles for rivaroxaban 5 and 10 mg with the adjusted permeability coefficients were sufficiently reliable compared with experimental data. A slight trend towards an overestimation of time to reach maximum (peak) plasma concentration following drug administration (t_{max}) was observed in the simulations compared with the experimental data. After administration of the 10 mg dose, a slight underestimation of the plasma concentration measured 24 h after administration (C_{24h}) value was evident. Experimental data for this time point were not available for the 5 mg dose.

The effect of the dissolution behaviour of rivaroxaban immediate-release tablets on the area under the plasma concentration–time curve (AUC) was considered by using an add-on dissolution module of PK-Sim® for simulations of drug particle administration. The monodisperse particle dissolution parameters were optimised by comparing simulated plasma AUC with experimental data that were obtained after administration of tablets containing rivaroxaban 10 or 20 mg to fasted healthy volunteers. A diffusion coefficient of 4.9×10^{-5} cm^2/s was determined by fitting the simulated curves to the experimental data. Fitting this parameter resulted in a good fit of the simulated and the experimental plasma AUC (data not shown).

As a next step, this model was qualified using independent clinical study data.

3.1.3 Model Qualification

To qualify the PBPK model for oral tablet administration, independent data sets obtained from several phase I studies that assessed the pharmacokinetics of rivaroxaban 10 and 20 mg administered as tablets in healthy adults under fasted and fed conditions were compared with the corresponding simulation (Fig. 3). These results showed that, overall, the adult PBPK model is well suited to describe the pharmacokinetics of rivaroxaban after oral tablet administration under fasted and fed conditions. The majority of individual data points observed experimentally were within the 90 % prediction interval (Fig. 3). The model, however, tended to underestimate maximum (peak) plasma drug concentration (C_{max}) slightly and to overestimate t_{max} for some individuals after receiving tablets under fasted conditions. The C_{24h} values were uniformly distributed around the simulated geometric mean and were all confined within the 90 % prediction interval of the virtual population. In the fed state, most of the observed data points were located between the simulated geometric mean and the predicted 90 % percentile of the population. There was a slight mismatch between simulated and observed plasma concentrations after intake of rivaroxaban 10 or 20 mg with food, indicating that the distinct lag time observed in some individuals after administration of the immediate-release tablet under fed conditions was not adequately represented in the model.

Model predictions were also compared with data obtained from a phase I study that assessed the bioavailability of the suspension formulation intended for future clinical use in paediatric studies [32]. The plasma concentration–time profiles for rivaroxaban 10 and 20 mg suspension formulations administered under fasted conditions and 20 mg suspension under fed conditions were well described by the model as assessed by VPC. Most experimental data points were within the 90 % prediction interval, leading to a good agreement between simulated and experimental data. A slight trend towards underestimating the inter-individual variability was evident. The considerable delay in the absorption of tablet formulations when taken with food was not observed for the absorption of the suspension. In summary, these results demonstrate that the pharmacokinetics of rivaroxaban after oral administration of a tablet or suspension under fasted and fed conditions are well described by the PBPK model that was adjusted for gastrointestinal transit and absorption.

3.2 Paediatric PBPK Model of Rivaroxaban

For simulations in the paediatric population, doses of rivaroxaban (oral suspension formulation) were weight-adjusted to yield a low dose and a high dose equivalent to rivaroxaban 10 mg/70 kg body weight (0.143 mg/kg body weight) and rivaroxaban 20 mg/70 kg body weight (0.286 mg/kg body weight) in adults. Apart from anthropometric differences, there were no differences in simulations for male and female children and, therefore, sex-specific simulations were pooled (Fig. 4a–f).

Simulations with the paediatric PBPK model for the low dose and the high dose (corrected for body weight) resulted in similar graphs for C_{max}, AUC and C_{24h} values versus body weight (Fig. 4a–f). As expected, the values for these pharmacokinetic parameters with the high dose were consistently higher than the low dose. For both doses, simulated C_{max}, AUC and C_{24h} values for infants and children up to 40 kg body weight were much lower than the 90 % confidence interval (CI) of the adult reference population (Fig. 4a–f): the effect was most

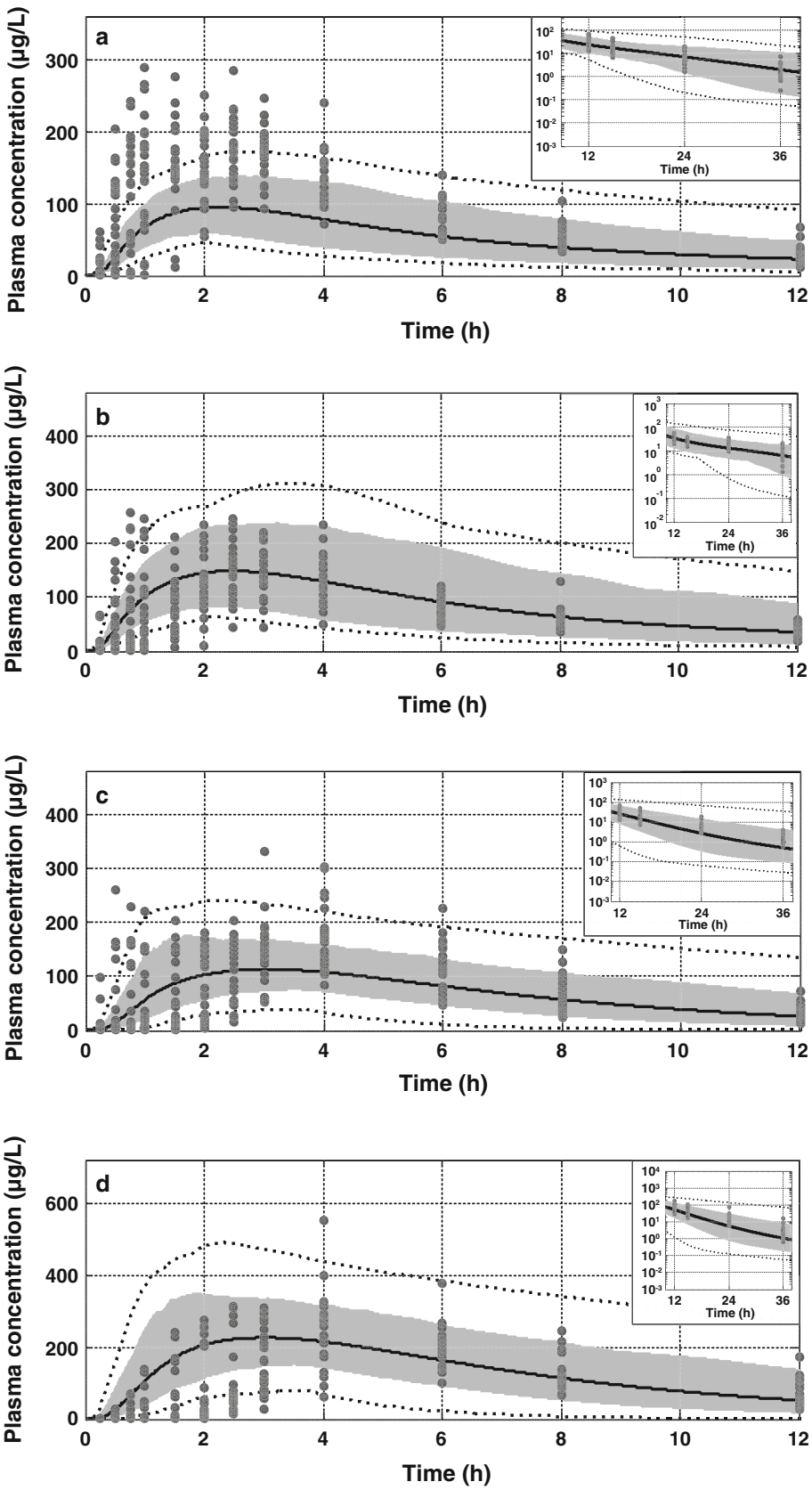

Fig. 3 Individually observed (*dots*) and simulated (*lines*) plasma concentration–time profiles for rivaroxaban after oral administration of an immediate-release tablet to healthy adults depicted as a linear (*main graph*) and semi-log plot (*inset*). Simulated data are represented as geometric means (*black line*), 90 % prediction interval (*grey shaded area*) and minimum and maximum values (*dotted lines*). The graphs show concentration–time profiles of 10 mg (**a**, **c**) and 20 mg (**b**, **d**) rivaroxaban, under fasting (**a**, **b**) and fed (**c**, **d**) conditions

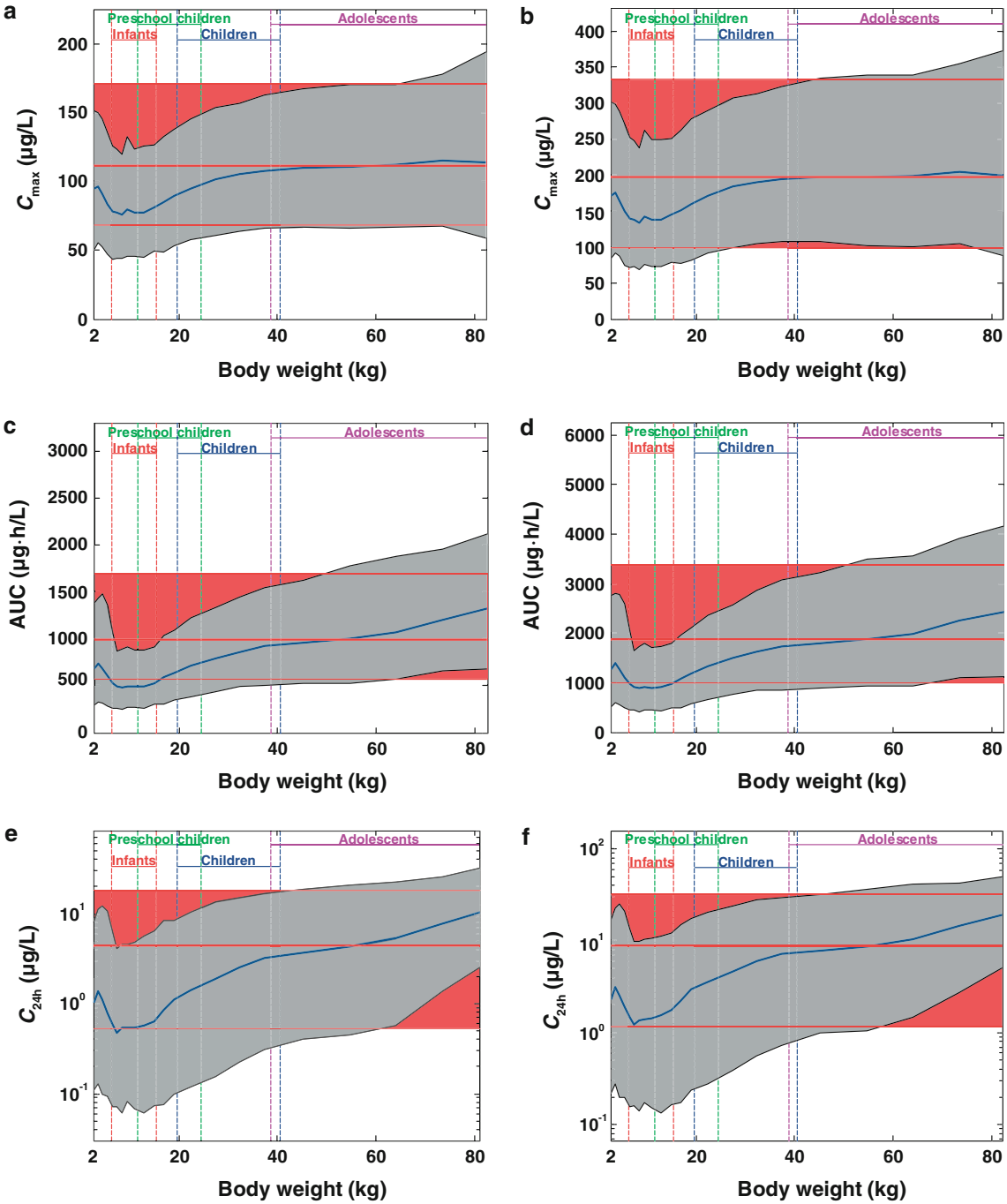

Fig. 4 Gender-pooled paediatric simulations for maximum (peak) plasma drug concentration (C_{max}) (**a**, **b**), area under the plasma concentration–time curve (AUC) (**c**, **d**) and concentration in plasma after 24 h (C_{24h}) (**e**, **f**) versus body weight for two different doses of rivaroxaban: 0.143 mg/kg body weight (**a**, **c**, **e**) and 0.286 mg/kg body weight (**b**, **d**, **f**), simulated as oral suspension formulation compared with the adult reference population. Simulated data of the paediatric population are represented as geometric means (*blue line*) and 90 % prediction interval (*grey shaded area*). Simulated data of the adult reference population are represented as geometric means (*thick red line*) and 90 % confidence interval (*red shaded area* in the background of the graph). Expected body weight ranges for infants, preschool children, children and adolescents are indicated

pronounced for C_{24h} values. In children with higher body weight and in adults of >70 kg body weight, the simulated 90 % prediction interval values of AUC and C_{24h} were much higher than the 90 % CI of the adult reference population, but this is not the case for the simulated C_{max} values (Fig. 4a, b).

The predicted geometric means of C_{max}, AUC and C_{24h} values for all simulated age groups and both doses were located within the 90 % CI of the adult reference population. However, a trend towards lower mean plasma exposures and trough concentrations of rivaroxaban can be observed in preschool children and infants (body weight below 40 kg).

4 Discussion

An established workflow for PBPK-based scaling from adults to children was used for the prediction of rivaroxaban pharmacokinetics in children. Based on extensive clinical data, the adult reference model could successfully be parameterised. Parameters that were adjusted based on the experimental data sets obtained in adults include the lipophilicity and the diffusion coefficient for the monodisperse particle dissolution. It is noteworthy that the intravenous administration in the absolute bioavailability study was purely of an experimental nature and that rivaroxaban is only to be used as an oral formulation in clinical practice. In addition, phase I studies in healthy male adults demonstrated that there was no difference between suspension and tablet formulations of rivaroxaban with respect to pharmacokinetic parameters and bioavailability [32]; this is in part because both formulations contain the same micronised drug. The model accounts for different permeability parameters in the small and large intestine in a novel model for gastrointestinal transit and absorption. An important aspect of this PBPK model is that absorption from the large intestine is considered, because, unlike many other oral substances, the large intestine contributes significantly to the overall absorption of rivaroxaban. After successful development of the adult reference model, the PBPK model was scaled for children based on anatomical, physiological and developmental information.

The body weight-related dosing regimen led to a large overlap of the simulated plasma pharmacokinetic parameters (C_{max}, C_{24h} and AUC) for all age ranges with the values obtained in the corresponding adult reference simulation. Importantly, C_{24h} is the lowest concentration in a once-daily dosing regimen, and thus is an important parameter to assess efficacy and an important driver in the decision for paediatric dosing. Paediatric dosing should achieve pharmacokinetic profiles within the 90 % CI of the adult reference model, and simulated C_{24h} values should not drop below the threshold of the 90 % CI. Therefore, especially in infants and preschool children (body weight below 40 kg), the simulated dose with respect to body weight is too low as indicated by C_{24h} values close or below the 90 % CI threshold. This result indicates that dosing for these children would need to be increased to achieve pharmacokinetics similar to those in the adult population. For older children, simulated plasma pharmacokinetic parameters (C_{max}, C_{24h} and AUC) overlapped with the values obtained in the corresponding adult reference simulation, indicating that body weight-related exposure was similar between these children and adults. In children with higher body weight and in adults of >70 kg body weight, the simulated 90 % prediction interval values of AUC and C_{24h} were much higher than the 90 % CI of the adult reference population owing to the simulations for children being based on weight-dependent dosing (i.e. rivaroxaban mg/kg body weight). This resulted in an overestimation of dosing for heavier body weights because the adult reference population takes into account those patients with body weight ≥70 kg who receive fixed 10 or 20 mg doses of rivaroxaban (not weight adjusted).

In adults, rivaroxaban 10 mg can be taken with or without food, but the 20 mg dose should be taken with food to achieve high oral bioavailability [32]. The assumption of children being 50 % fed and 50 % fasted reflected the proposed study design for the ongoing phase I study (NCT01145859) and is in line with guidelines for the design of paediatric studies [88]. This is the first study to investigate rivaroxaban in paediatric patients, and is designed to explore the pharmacokinetic and pharmacodynamic profile of single doses of rivaroxaban in patients (aged between 6 months and 18 years) at the end of VTE treatment.

One potential limitation of the developed paediatric model is that it is based on the assumption of a normal, healthy development (especially with respect to organ development of the liver and kidney). Therefore, the model may be used to inform dosing in healthy children who require a major surgery and hence will be at risk of VTE. In adults, in the first 2 postoperative days caution is recommended because the pharmacokinetics of rivaroxaban are more variable than at steady state [89]; this may also be the case in children. The proposed model does not account for the effects of comorbidities, such as cystic fibrosis or cancer, or other conditions that could potentially influence rivaroxaban exposure. Developmental delays that will affect the pharmacokinetics of rivaroxaban in children have to be taken into account when considering body weight-related dosing.

By definition, traditional compartmental modelling approaches have limited predictive capability because they will not account for all of the physiological, anatomical and/or biochemical changes associated with development, nor for how the absorption, distribution, metabolism and excretion of the drug may be affected by these changes [33]. As described in this article, the paediatric PBPK model for rivaroxaban takes into account various developmental changes including changes in gastrointestinal physiology and motility (see Table 3 and Methods section).

This PBPK scaling approach allowed an exploratory analysis of the pharmacokinetics of rivaroxaban in children to inform the dosing regimen for the clinical study in paediatric patients. It will also be interesting to investigate the pharmacodynamics of rivaroxaban in children. In adults, there is a good correlation between the pharmacokinetics and pharmacodynamics of rivaroxaban, with parameters such as Factor Xa inhibition and prolongation of prothrombin time being closely correlated with plasma concentrations of rivaroxaban [15, 16, 90, 91]. Such correlations are expected also to apply to the paediatric population.

5 Conclusions

The pharmacokinetic properties of rivaroxaban in children have been simulated for two body weight-related dosing regimens equivalent to 10 and 20 mg once daily in adults using a newly developed paediatric PBPK model. Simulations for AUC, C_{max} and C_{24h} with respect to body weight as an indicator for age showed a large overlap with values obtained for the corresponding dose in the adult reference simulation. However, pharmacokinetic values in infants and preschool children were lower than the 90 % CI threshold of the adult reference model, indicating that doses in these children may need to be increased to achieve the desired pharmacokinetic profile. This PBPK scaling approach allowed an exploratory analysis of the pharmacokinetics of rivaroxaban in children to inform the dosing regimen for the clinical study in paediatric patients.

Acknowledgments The authors would like to acknowledge Claudia Wiedemann, who provided editorial support with funding from Bayer HealthCare Pharmaceuticals. The authors declare that CB, RB, KC, JL, WM, H-US, KT and SW are employees of Bayer Technology Services or Bayer HealthCare. AE was a Bayer employee from 2004 to 2008. The employees of Bayer Technology Services and Bayer HealthCare are potential stockholders of Bayer AG.

References

1. Raffini L, Huang YS, Witmer C, et al. Dramatic increase in venous thromboembolism in children's hospitals in the United States from 2001 to 2007. Pediatrics. 2009;124:1001–8.
2. Goldenberg NA, Donadini MP, Kahn SR, et al. Post-thrombotic syndrome in children: a systematic review of frequency of occurrence, validity of outcome measures, and prognostic factors. Haematologica. 2010;95:1952–9.
3. Kuhle S, Massicotte P, Chan A, et al. Systemic thromboembolism in children. Data from the 1-800-NO-CLOTS Consultation Service. Thromb Haemost. 2004;92:722–8.
4. Rosendaal FR. Thrombosis in the young: epidemiology and risk factors. A focus on venous thrombosis. Thromb Haemost. 1997;78:1–6.
5. van Ommen CH, Heijboer H, Büller HR, et al. Venous thromboembolism in childhood: a prospective two-year registry in The Netherlands. J Pediatr. 2001;139:676–81.
6. Andrew M, David M, Adams M, et al. Venous thromboembolic complications (VTE) in children: first analyses of the Canadian Registry of VTE. Blood. 1994;83:1251–7.
7. Streif W, Ageno W. Direct thrombin and Factor Xa inhibitors in children: a quest for new anticoagulants for children. Wien Med Wochenschr. 2011;161:73–9.
8. Monagle P, Chan AK, Goldenberg NA, et al. Antithrombotic therapy in neonates and children: antithrombotic therapy and prevention of thrombosis, 9th ed: American College of Chest Physicians evidence-based clinical practice guidelines. Chest. 2012;141:e737S–801S.
9. Conroy S, McIntyre J. The use of unlicensed and off-label medicines in the neonate. Semin Fetal Neonatal Med. 2005;10:115–22.
10. Choonara I. Unlicensed and off-label drug use in children: implications for safety. Expert Opin Drug Saf. 2004;3:81–3.
11. Conroy S, Choonara I, Impicciatore P, et al. Survey of unlicensed and off label drug use in paediatric wards in European countries. European Network for Drug Investigation in Children. BMJ. 2000;320:79–82.
12. Cuzzolin L, Atzei A, Fanos V. Off-label and unlicensed prescribing for newborns and children in different settings: a review of the literature and a consideration about drug safety. Expert Opin Drug Saf. 2006;5:703–18.
13. 't Jong GW, Vulto AG, de Hoog M, et al. A survey of the use of off-label and unlicensed drugs in a Dutch children's hospital. Pediatrics. 2001;108:1089–93.
14. Roberts R, Rodriguez W, Murphy D, et al. Pediatric drug labeling: improving the safety and efficacy of pediatric therapies. JAMA. 2003;290:905–11.
15. Kubitza D, Becka M, Wensing G, et al. Safety, pharmacodynamics, and pharmacokinetics of BAY 59-7939—an oral, direct Factor Xa inhibitor—after multiple dosing in healthy male subjects. Eur J Clin Pharmacol. 2005;61:873–80.
16. Kubitza D, Becka M, Voith B, et al. Safety, pharmacodynamics, and pharmacokinetics of single doses of BAY 59-7939, an oral, direct Factor Xa inhibitor. Clin Pharmacol Ther. 2005;78:412–21.
17. Kubitza D, Becka M, Zuehlsdorf M, et al. No interaction between the novel, oral direct Factor Xa inhibitor BAY 59-7939 and digoxin [abstract no. 11]. J Clin Pharmacol. 2006;46:702.
18. Kubitza D, Becka M, Zuehlsdorf M, et al. Effect of food, an antacid, and the H2 antagonist ranitidine on the absorption of BAY 59-7939 (rivaroxaban), an oral, direct Factor Xa inhibitor, in healthy subjects. J Clin Pharmacol. 2006;46:549–58.
19. Kubitza D, Becka M, Mueck W, et al. Safety, tolerability, pharmacodynamics, and pharmacokinetics of rivaroxaban—an oral, direct Factor Xa inhibitor—are not affected by aspirin. J Clin Pharmacol. 2006;46:981–90.
20. Kubitza D, Becka M, Mueck W, et al. Rivaroxaban (BAY 59-7939)—an oral, direct Factor Xa inhibitor—has no clinically relevant interaction with naproxen. Br J Clin Pharmacol. 2007;63:469–76.
21. Kubitza D, Mueck W, Becka M. No interaction between rivaroxaban—a novel, oral, direct Factor Xa inhibitor—and atorvastatin [abstract no. P062]. Pathophysiol Haemost Thromb. 2008;36:A40.
22. Kubitza D, Becka M, Mueck W, et al. Effect of co-administration of rivaroxaban and clopidogrel on bleeding time, pharmacodynamics

and pharmacokinetics: a phase I study. Pharmaceuticals. 2012;5: 279–96.
23. Perzborn E, Roehrig S, Straub A, et al. The discovery and development of rivaroxaban, an oral, direct Factor Xa inhibitor. Nat Rev Drug Discov. 2011;10:61–75.
24. Eriksson BI, Borris LC, Friedman RJ, et al. Rivaroxaban versus enoxaparin for thromboprophylaxis after hip arthroplasty. N Engl J Med. 2008;358:2765–75.
25. Kakkar AK, Brenner B, Dahl OE, et al. Extended duration rivaroxaban versus short-term enoxaparin for the prevention of venous thromboembolism after total hip arthroplasty: a double-blind, randomised controlled trial. Lancet. 2008;372:31–9.
26. Lassen MR, Ageno W, Borris LC, et al. Rivaroxaban versus enoxaparin for thromboprophylaxis after total knee arthroplasty. N Engl J Med. 2008;358:2776–86.
27. Turpie AGG, Lassen MR, Davidson BL, et al. Rivaroxaban versus enoxaparin for thromboprophylaxis after total knee arthroplasty (RECORD4): a randomised trial. Lancet. 2009;373: 1673–80.
28. The EINSTEIN Investigators. Oral rivaroxaban for symptomatic venous thromboembolism. N Engl J Med. 2010;363:2499–510.
29. The EINSTEIN-PE Investigators. Oral rivaroxaban for the treatment of symptomatic pulmonary embolism. N Engl J Med. 2012;366:1287–97.
30. Patel MR, Mahaffey KW, Garg J, et al. Rivaroxaban versus warfarin in nonvalvular atrial fibrillation. N Engl J Med. 2011;365:883–91.
31. Mega JL, Braunwald E, Wiviott SD, et al. Rivaroxaban in patients with a recent acute coronary syndrome. N Engl J Med. 2012;366:9–19.
32. Stampfuss J, Kubitza D, Becka M, et al. The effect of food on the absorption and pharmacokinetics of rivaroxaban. Int J Clin Pharmacol Ther. 2013;51:549–61.
33. Strougo A, Eissing T, Yassen A, et al. First dose in children: physiological insights into pharmacokinetic scaling approaches and their implications in paediatric drug development. J Pharmacokinet Pharmacodyn. 2012;39:195–203.
34. Edginton AN, Schmitt W, Willmann S. Development and evaluation of a generic physiologically based pharmacokinetic model for children. Clin Pharmacokinet. 2006;45:1013–34.
35. Zhao P, Zhang L, Grillo JA, et al. Applications of physiologically based pharmacokinetic (PBPK) modeling and simulation during regulatory review. Clin Pharmacol Ther. 2011;89:259–67.
36. Leong R, Vieira ML, Zhao P, et al. Regulatory experience with physiologically based pharmacokinetic modeling for pediatric drug trials. Clin Pharmacol Ther. 2012;91:926–31.
37. Weinz C, Schwarz T, Kubitza D, et al. Metabolism and excretion of rivaroxaban, an oral, direct Factor Xa inhibitor, in rats, dogs and humans. Drug Metab Dispos. 2009;37:1056–64.
38. Edginton AN. Knowledge-driven approaches for the guidance of first-in-children dosing. Paediatr Anaesth. 2011;21:206–13.
39. Thelen K, Coboeken K, Willmann S, et al. Evolution of a detailed physiological model to simulate the gastrointestinal transit and absorption process in humans, part 1: oral solutions. J Pharm Sci. 2011;100:5324–45.
40. Thelen K, Coboeken K, Willmann S, et al. Evolution of a detailed physiological model to simulate the gastrointestinal transit and absorption process in humans, part II: extension to describe performance of solid dosage forms. J Pharm Sci. 2012;101: 1267–80.
41. Rodgers T, Leahy D, Rowland M. Physiologically based pharmacokinetic modeling 1: predicting the tissue distribution of moderate-to-strong bases. J Pharm Sci. 2005;94:1259–76.
42. Rodgers T, Rowland M. Physiologically based pharmacokinetic modelling 2: predicting the tissue distribution of acids, very weak bases, neutrals and zwitterions. J Pharm Sci. 2006;95:1238–57.
43. Rodgers T, Rowland M. Mechanistic approaches to volume of distribution predictions: understanding the processes. Pharm Res. 2007;24:918–33.
44. Kubitza D, Becka M, Mueck W, et al. Effects of renal impairment on the pharmacokinetics, pharmacodynamics and safety of rivaroxaban, an oral, direct Factor Xa inhibitor. Br J Clin Pharmacol. 2010;70:703–12.
45. Bayer Pharma AG. Xarelto® (rivaroxaban) summary of product characteristics; 2013. http://www.ema.europa.eu/docs/en_GB/document_library/EPAR_-_Product_Information/human/000944/WC500057108.pdf (Accessed 22 May 2013).
46. Kubitza D, Roth A, Becka M, et al. Effect of hepatic impairment on the pharmacokinetics and pharmacodynamics of a single dose of rivaroxaban—an oral, direct Factor Xa inhibitor. Br J Clin Pharmacol. 2013;76:89–98.
47. Gryback P, Hermansson G, Lyrenas E, et al. Nationwide standardisation and evaluation of scintigraphic gastric emptying: reference values and comparisons between subgroups in a multicentre trial. Eur J Nucl Med. 2000;27:647–55.
48. Thelen K, Coboeken K, Jia Y, et al. Dynamically simulating the effect of food on gastric emptying using a detailed physiological model for gastrointestinal transit and absorption [abstract no. II-36]. Population Approach Group Europe, Venice; 2012.
49. Johnson KC. Dissolution and absorption modeling: model expansion to simulate the effects of precipitation, water absorption, longitudinally changing intestinal permeability, and controlled release on drug absorption. Drug Dev Ind Pharm. 2003;29:833–42.
50. Willmann S, Thelen K, Becker C, et al. Mechanism-based prediction of particle size-dependent dissolution and absorption: cilostazol pharmacokinetics in dogs. Eur J Pharm Biopharm. 2010;76:83–94.
51. Post TM, Freijer JI, Ploeger BA, et al. Extensions to the visual predictive check to facilitate model performance evaluation. J Pharmacokinet Pharmacodyn. 2008;35:185–202.
52. Bergstrand M, Hooker AC, Wallin JE, et al. Prediction-corrected visual predictive checks for diagnosing nonlinear mixed-effects models. AAPS J. 2011;13:143–51.
53. Edginton AN, Schmitt W, Voith B, et al. A mechanistic approach for the scaling of clearance in children. Clin Pharmacokinet. 2006;45:683–704.
54. Pang KS, Rowland M. Hepatic clearance of drugs. I. Theoretical considerations of a "well-stirred" model and a "parallel tube" model. Influence of hepatic blood flow, plasma and blood cell binding, and the hepatocellular enzymatic activity on hepatic drug clearance. J Pharmacokinet Biopharm. 1977;5:625–53.
55. Edginton AN, Willmann S. Physiology-based simulations of a pathological condition: prediction of pharmacokinetics in patients with liver cirrhosis. Clin Pharmacokinet. 2008;47:743–52.
56. McNamara PJ, Alcorn J. Protein binding predictions in infants. AAPS Pharm Sci. 2002;4:E4.
57. Mahmood B, Daood MJ, Hart C, et al. Ontogeny of P-glycoprotein in mouse intestine, liver, and kidney. J Investig Med. 2001;49:250–7.
58. Rosati A, Maniori S, Decorti G, et al. Physiological regulation of P-glycoprotein, MRP1, MRP2 and cytochrome P450 3A2 during rat ontogeny. Dev Growth Differ. 2003;45:377–87.
59. Pinto N, Halachmi N, Verjee Z, et al. Ontogeny of renal P-glycoprotein expression in mice: correlation with digoxin renal clearance. Pediatr Res. 2005;58:1284–9.
60. Wagner JG. Inter- and intrasubject variation of digoxin renal clearance in normal adult males. Drug Intell Clin Pharm. 1988;22:562–7.
61. MacFarland RT, Moeller VR, Pieniaszek HJ Jr, et al. Assessment of the potential pharmacokinetic interaction between digoxin and ethmozine. J Clin Pharmacol. 1985;25:138–43.

62. Gorodischer R, Jusko WJ, Yaffe SJ. Renal clearance of digoxin in young infants. Res Commun Chem Pathol Pharmacol. 1977;16: 363–74.
63. Halkin H, Radomsky M, Millman P, et al. Steady state serum concentrations and renal clearance of digoxin in neonates, infants and children. Eur J Clin Pharmacol. 1978;13:113–7.
64. Collins-Nakai RL, Schiff D, Ng PK. Multiple-dose kinetics of digoxin in neonates. Pediatr Pharmacol (New York). 1985;5: 117–22.
65. Iisalo E, Dahl M. Serum levels and renal excretion of digoxin during maintenance therapy in children. Acta Paediatr Scand. 1974;63:699–704.
66. Willmann S, Lippert J, Schmitt W. From physicochemistry to absorption and distribution: predictive mechanistic modelling and computational tools. Expert Opin Drug Metab Toxicol. 2005;1:159–68.
67. Willmann S, Hohn K, Edginton A, et al. Development of a physiology-based whole-body population model for assessing the influence of individual variability on the pharmacokinetics of drugs. J Pharmacokinet Pharmacodyn. 2007;34:401–31.
68. Damkier P, Brosen K. Quinidine as a probe for CYP3A4 activity: intrasubject variability and lack of correlation with probe-based assays for CYP1A2, CYP2C9, CYP2C19, and CYP2D6. Clin Pharmacol Ther. 2000;68:199–209.
69. Gaedigk A, Baker DW, Totah RA, et al. Variability of CYP2J2 expression in human fetal tissues. J Pharmacol Exp Ther. 2006;319:523–32.
70. Rhodin MM, Anderson BJ, Peters AM, et al. Human renal function maturation: a quantitative description using weight and postmenstrual age. Pediatr Nephrol. 2009;24:67–76.
71. Dorne JL, Walton K, Renwick AG. Human variability in CYP3A4 metabolism and CYP3A4-related uncertainty factors for risk assessment. Food Chem Toxicol. 2003;41:201–24.
72. Sy SK, Ciaccia A, Li W, et al. Modeling of human hepatic CYP3A4 enzyme kinetics, protein, and mRNA indicates deviation from log-normal distribution in CYP3A4 gene expression. Eur J Clin Pharmacol. 2002;58:357–65.
73. Garzi A, Messina M, Frati F, et al. An extensively hydrolysed cow's milk formula improves clinical symptoms of gastro-esophageal reflux and reduces the gastric emptying time in infants. Allergol Immunopathol (Madr). 2002;30:36–41.
74. Shaaban SY, Nassar MF, Sawaby AS, et al. Ultrasonographic gastric emptying in protein energy malnutrition: effect of type of meal and nutritional recovery. Eur J Clin Nutr. 2004;58:972–8.
75. Vivatvakin B, Buachum V. Effect of carob bean on gastric emptying time in Thai infants. Asia Pac J Clin Nutr. 2003;12:193–7.
76. Fallingborg J, Christensen LA, Ingeman-Nielsen M, et al. Measurement of gastrointestinal pH and regional transit times in normal children. J Pediatr Gastroenterol Nutr. 1990;11:211–4.
77. Ofori-Kwakye K, Fell JT, Sharma HL, et al. Gamma scintigraphic evaluation of film-coated tablets intended for colonic or biphasic release. Int J Pharm. 2004;270:307–13.
78. Hoekstra JH. Fructose breath hydrogen tests in infants with chronic non-specific diarrhoea. Eur J Pediatr. 1995;154:362–4.
79. Khin M, Bolin TD, Tin O, et al. Investigation of small-intestinal transit time in normal and malnourished children. J Gastroenterol. 1999;34:675–9.
80. Soares AC, Lederman HM, Fagundes-Neto U, et al. Breath hydrogen test after a bean meal demonstrates delayed oro-cecal transit time in children with chronic constipation. J Pediatr Gastroenterol Nutr. 2005;41:221–4.
81. Van Den Driessche M, Van Malderen N, Geypens B, et al. Lactose-[13C]ureide breath test: a new, noninvasive technique to determine orocecal transit time in children. J Pediatr Gastroenterol Nutr. 2000;31:433–8.
82. Vreugdenhil G, Sinaasappel M, Bouquet J. A comparative study of the mouth to caecum transit time in children and adults using a weight adapted lactulose dose. Acta Paediatr Scand. 1986;75:483–8.
83. Madsen JL. Effects of gender, age, and body mass index on gastrointestinal transit times. Dig Dis Sci. 1992;37:1548–53.
84. Wagener S, Shankar KR, Turnock RR, et al. Colonic transit time—what is normal? J Pediatr Surg. 2004;39:166–9.
85. Helander HF. Quantitative morphological methods in intestinal research. Scand J Gastroenterol Suppl. 1985;112:1–5.
86. Willmann S, Edginton AN, Kleine-Besten M, et al. Whole-body physiologically based pharmacokinetic population modelling of oral drug administration: inter-individual variability of cimetidine absorption. J Pharm Pharmacol. 2009;61:891–9.
87. Wilding I, Hirst P, Connor A. Development of a new engineering-based capsule for human drug absorption studies. Pharm Sci Technol Today. 2000;3:385–92.
88. US Department of Health and Human Services Food and Drug Administration Center for Drug Evaluation and Research (CDER). General considerations for pediatric pharmacokinetic studies for drugs and biological products; 1998. http://www.fda.gov/downloads/Drugs/GuidanceComplianceRegulatoryInformation/Guidances/ucm072114.pdf (Accessed 19 Mar 2013).
89. Mueck W, Borris LC, Dahl OE, et al. Population pharmacokinetics and pharmacodynamics of once- and twice-daily rivaroxaban for the prevention of venous thromboembolism in patients undergoing total hip replacement. Thromb Haemost. 2008;100: 453–61.
90. Mueck W, Becka M, Kubitza D, et al. Population model of the pharmacokinetics and pharmacodynamics of rivaroxaban—an oral, direct Factor Xa inhibitor—in healthy subjects. Int J Clin Pharmacol Ther. 2007;45:335–44.
91. Mueck W, Lensing AW, Agnelli G, et al. Rivaroxaban: population pharmacokinetic analyses in patients treated for acute deep-vein thrombosis and exposure simulations in patients with atrial fibrillation treated for stroke prevention. Clin Pharmacokinet. 2011;50:675–86.